Analysis of Spatiotemporal Changes in Land Cover of Wind Farms within County Areas

Ting Liu[1], Tao Zhang[1]*, Guanghui Wang[1], Yunjia Zou[1], Wei Zhang[1], Hailun Dai[1,2]

[1] Land Satellite Remote Sensing Application Center, MNR, Beijing, China - liuting@lasac.cn, zhangt@lasac.cn, wanggh@lasac.cn, zouyunjia@lasac.cn, zhangwei@lasac.cn

[2] Beijing Satlmage Information Technology Co. Ltd., Beijing, China - 99261010@qq.com

Keywords: Wind farms, Land cover, Spatiotemporal changes, Environmental impact.

Abstract

The rapid expansion of wind energy has raised growing concerns about its impacts on land cover and the environment. This study focuses on county-level areas with high-density wind farm distribution in the Xing'an League, Inner Mongolia, China. Using high-resolution satellite imagery from 2016 to 2024, we visually interpreted land cover within and around wind farms and analyzed their spatiotemporal dynamics. The results show that: (1) Land cover change in the study area was primarily driven by wind farm expansion, which increased by 130.87 km² (+260.35%) from 2016 to 2024, exhibiting the highest dynamic degree among all land cover categories (LK = +32.54%/yr). (2) Grassland was the most affected land cover type, with 78.74 km² converted to wind farm land, accounting for 59.66% of newly established wind farm area, followed by cultivated land (20.06%) and forest land (18.33%). (3) With wind power expansion, the land cover composition within wind farms shifted from a cultivated land–grassland balance toward grassland dominance. (4) Areas temporarily disturbed by wind farm construction tended to recover progressively, with cultivated land recovering faster than grassland. These findings provide an important basis for assessing the environmental impacts of wind farm development in Inner Mongolia.

1. Introduction

The escalating global energy demand, coupled with urgent commitments to carbon neutrality, has accelerated the transition from fossil fuels toward renewable energy sources. Among these, wind energy has emerged as one of the most technically mature and cost-effective options, playing an increasingly vital role in national energy strategies worldwide (Kumar et al., 2025; Liu et al., 2022). China has witnessed remarkable growth in its wind power sector over the past decade. Driven by supportive national policies and substantial capital investment, China's cumulative installed wind power capacity has grown dramatically, making it the world's largest wind energy market (IEA, 2024; Liu et al., 2024). Nowhere is this expansion more pronounced than in Inner Mongolia, where vast, unobstructed plains and consistently high wind speeds provide ideal conditions for large-scale wind farm development. Inner Mongolia has ranked first in China in terms of installed wind power capacity for many consecutive years, and its wind farms continue to proliferate at a rapid pace. While this growth undeniably contributes to regional economic development and national decarbonization goals, it also raises growing concerns about its environmental footprint—particularly with respect to land use and ecosystem integrity.

Wind farm construction entails a range of land interventions, from the direct occupation of surface area by turbine foundations, access roads, and substations, to the indirect disturbance of surrounding land cover during the construction phase, such as grassland, forest, and cultivated land. Studies have documented that these interventions can fragment habitats, alter soil properties, affect local biodiversity, and disrupt ecosystem services (Li et al., 2024; Korozi et al., 2024; Aristides et al., 2023; Zhang et al., 2022; Zhao et al., 2025). In particular, grassland ecosystems—such as those dominant in Inner Mongolia—are especially vulnerable, as wind farm construction has been shown to reduce plant community diversity, alter surface temperature regimes, and affect soil nutrient cycling (Zhao et al., 2025; Han et al., 2025; Fei et al., 2025). Moreover, large-scale wind farm development can induce landscape fragmentation, leading to measurable losses in ecosystem service value (Jia et al., 2024). However, systematic, quantitative assessments of how land cover changes over time in wind farm areas—especially at the county administrative scale—remain limited. Most existing studies either focus on site-level impacts in isolation or lack the temporal depth needed to capture post-construction ecological trajectories, including the extent and rate of vegetation recovery.

Remote sensing technology provides an efficient and cost-effective approach for monitoring land cover change at regional scales over extended time periods. High-resolution satellite imagery, combined with visual interpretation and classification methods, enables the accurate mapping of multiple land cover types and the quantification of conversion dynamics among them (Yang et al., 2016; Sun et al., 2024), Previous studies have applied remote sensing to assess wind farm impacts in various regions; however, analyses specifically targeting county-level areas with dense wind farm distribution over consecutive years remain limited. Most existing research either focuses on broader regional scales that may obscure local variation, or relies on coarse-resolution imagery insufficient to capture the fine-scale land alterations associated with turbine installation and road construction (Chen et al., 2025; Deng et al., 2025).

Therefore, this study focuses on county-level areas with high de-

This contribution has been peer-reviewed.

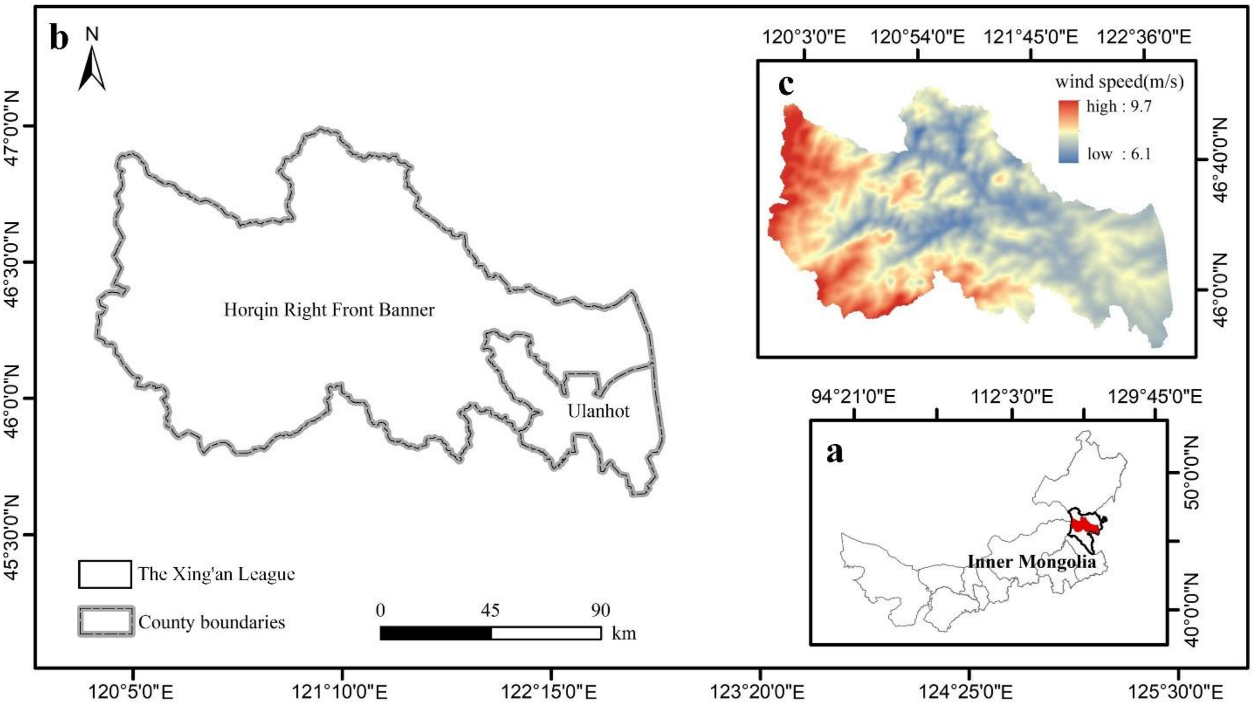

Figure 1. Study Area. (a) Geographical location; (b) The area of the two counties; (c) Wind speed.

Satellite	Sensor	Spatial Resolution	Temporal Coverage
GF-1	PMS/WFV	2 m (pan) / 8 m (MS)	2016–2022
GF-2	PMS/MS	2 m (pan) / 8 m (MS)	2016–2024
GF-7	DLIC	0.65 m (pan) / 2.6 m (MS)	2020–2024
ZY-3	MUX	2.1 m (pan) / 5.8 m (MS)	2016–2024

Table 1. Multi-source satellite data used in this study.

nsity wind farm distribution in the Xing'an League of Inner Mongolia. Using high-resolution satellite imagery from 2016 to 2024, we extracted land cover information around wind farms through visual interpretation. Based on the derived long-term land cover dataset, a statistical analysis was conducted to examine the spatiotemporal dynamics of land cover within county-scale wind farms and their surrounding areas. Specifically, this study aims to: (1) characterize the types and magnitudes of land cover changes attributable to wind farm development; (2) quantify the spatial extent of both direct and indirect surface disturbances; and (3) assess the degree of land cover restoration following wind farm construction. The findings are expected to provide a scientific basis for regional wind power development planning, ecological impact assessment, and the formulation of evidence-based environmental protection and restoration strategies.

2. Study Area

The study area comprises two counties in the Xing'an League of Inner Mongolia—Keerqin Right Wing Front Banner and Ulanhot— covering a total area of approximately 19,353 square kilometres (km^2), both characterized by abundant wind energy resources (Figure 1). The average annual wind speed at a hub height of 100 meters ranges from 5.6 to 8.5 m/s, with wind energy exhibiting a pronounced spatial concentration and no recorded occurrences of destructive wind events. These attributes, together with the region's relatively flat topography and favorable prevailing wind conditions, render it highly suitable for large-scale wind farm development. Over the past decade, driven by national renewable energy policies, the region's installed wind power capacity has expanded considerably. While this growth has contributed meaningfully to local economic development, the environmental implications are inherently twofold, as the construction and operation of wind farms also exert pressures on the local ecological environment. These competing dynamics underscore the need for systematic land cover monitoring in wind farm development areas.

3. Data and Methods

3.1 Data sources and processing

The study employed multi-source high-resolution remote sensing imagery from the Gaofen-1 (GF-1), Gaofen-2 (GF-2), Gaofen-7 (GF-7), and Ziyuan-3 (ZY-3) satellites with high spatial resolution (Table 1). The temporal coverage spans from 2016 to 2024, with image acquisition dates selected to coincide with the vegetation growing season (June–September) to minimize seasonal variability. The primary data processing steps included orthorectification, image registration, image fusion, and mosaicking and cropping. To ensure data quality, cloud cover was controlled to below 5%.

3.2 Land Cover Information Extraction

Land cover information was extracted through visual interpretation of fused high-resolution satellite imagery for five epochs spanning from 2016 to 2024 at two-year intervals. A classify-cation scheme comprising seven land cover categories was estab-

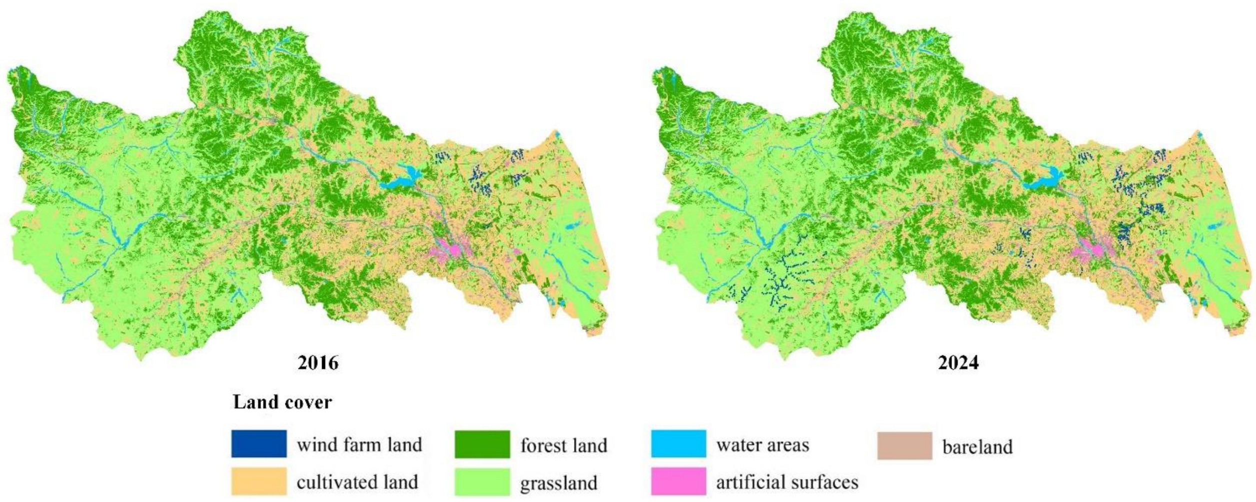

Figure 2. Land cover classification of the study area in 2016 and 2024.

lished: cultivated land, forest land, grassland, water area, artificial surface, bare land, and wind farm land. The "wind farm land" category—not commonly found in standard classification schemes—specifically delineates areas occupied by turbine foundations, associated infrastructure, and other disturbed zones, making it central to this study's objectives. To simplify the analytical process, a 300 m buffer zone around each turbine location was adopted to delineate the spatial extent of wind farm areas for statistical analysis and subsequent assessment (Denholm et al., 2009; Aydin et al., 2010).

To improve interpretation reliability, a multi-interpreter cross-validation workflow was implemented. Images at each time point were independently interpreted by multiple qualified remote sensing analysts following the same classification scheme. The resulting maps were then compared via overlay analysis to identify discrepancies; disputed parcels were resolved through collective review until consensus was reached. This iterative quality control procedure effectively reduces individual subjective bias and systematic interpretation errors.

3.3 Spatiotemporal Changes Analysis

To explore the spatiotemporal variations of land cover in the county where the wind farm is located from 2016 to 2024, we calculated the single land use dynamic attitude (LK) and the comprehensive land use type dynamic attitude (LC). The LK can reflect the speed and extent of change of different land cover types. A positive LK value indicates an expanding land cover type, while a negative value reflects a declining one. The magnitude of LK reflects the intensity of change: higher absolute values indicate more rapid transformations.

$$LK = \frac{U_b - U_a}{U_a} \times \frac{1}{t_2 - t_1} \times 100\%$$

where t = research period
U_a, U_b = the area of a certain land cover type at the beginning and end of the research respectively

The LC index integrates information across all land cover categories to reflect the overall rate of land cover transition within the entire study area.

$$LC = \left[\frac{\sum_{i=1}^{n} \Delta LU_{i-j}}{2\sum_{i=1}^{n} LU_i} \right] \times \frac{1}{t_2 - t_1} \times 100\%$$

where LU_i = the area of the land cover i at the beginning of the research
$\Delta LU_{i\text{-}j}$ = the area of land cover i converted into the land cover j during the research period
n = the total number of land cover types

To visualize and quantify the directionality and magnitude of conversions among different land cover types, a land cover transfer matrix was constructed for each consecutive time interval.

$$S_{ij} = \begin{bmatrix} S_{11} & \cdots & S_{1n} \\ \vdots & \ddots & \vdots \\ S_{n1} & \cdots & S_{nn} \end{bmatrix}$$

where n = the number of land cover types
S_{ij} = the area of land cover i at the beginning of the period that was converted to land cover type j by the end of the period.

4. Results and Analysis

4.1 Spatiotemporal Dynamics of Land Cover (2016–2024)

4.1.1 Overall Changes: Land cover data were extracted for the years 2016, 2018, 2020, 2022, and 2024 with the land cover maps for 2016 and 2024 presented in Figure 2. From 2016 to 2024, the composition of land cover classes underwent notable changes (Table 2). The comprehensive land use dynamic degree (LC) was calculated as +0.11%/yr, indicating a moderately active landscape transformation driven primarily by wind farm expansion. Wind farm land exhibited explosive growth, expanding from 50.27 km² in 2016 to 181.13 km² in 2024, representing a cumulative increase of 130.87 km² (+260.35%) and the highest dynamic degree among all categories (LK = +35.54/yr).

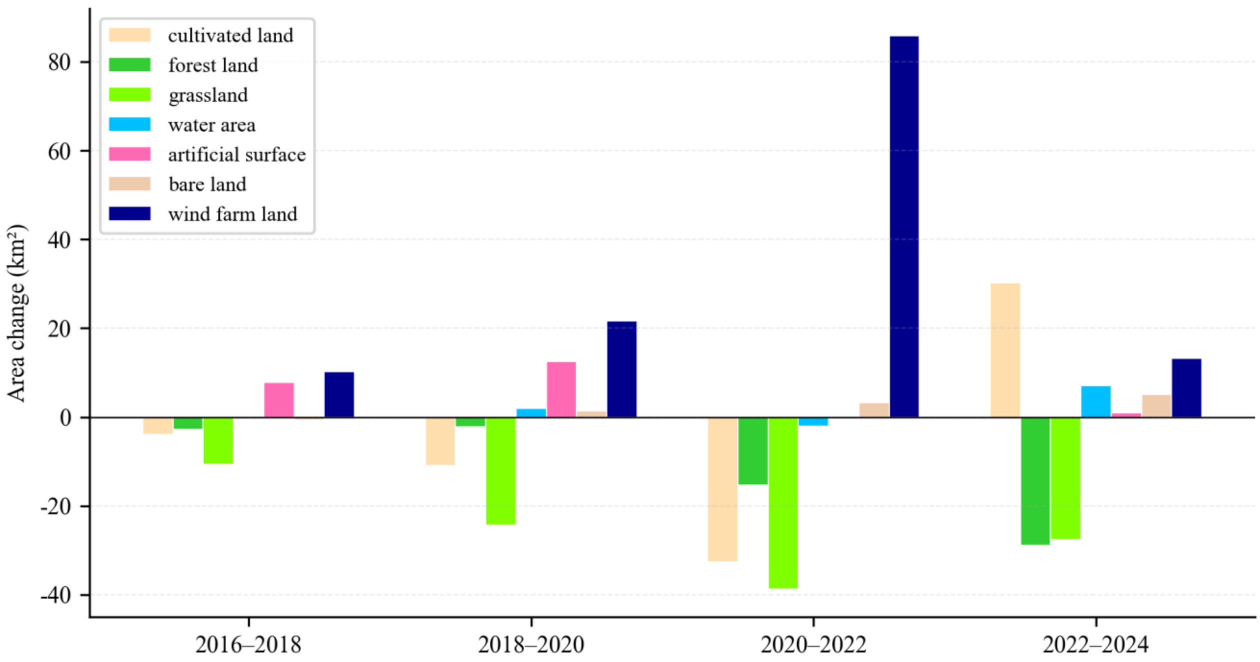

Figure 3. Period-by-Period Land Cover Changes.

Figure 4. Land cover transition matrix.

Land Class	2016 Area (km²)	2024 Area (km²)	Absolute Change (km²)	Percent Change (%)	LK (%/yr)
cultivated land	4971.31	4953.88	-17.44	-0.35	-0.04
forest land	4630.30	4581.12	-49.18	-1.06	-0.13
grassland	8348.70	8247.40	-101.29	-1.21	-0.15
water area	541.09	548.17	7.08	1.31	0.16
artificial surface	444.30	465.33	21.03	4.73	0.59
bare land	55.17	64.10	8.93	16.19	2.02
wind farm land	50.27	181.13	130.87	260.35	32.54

Table 2. Statistical metrics of each land cover type: area, area change, area change rate, and LK.

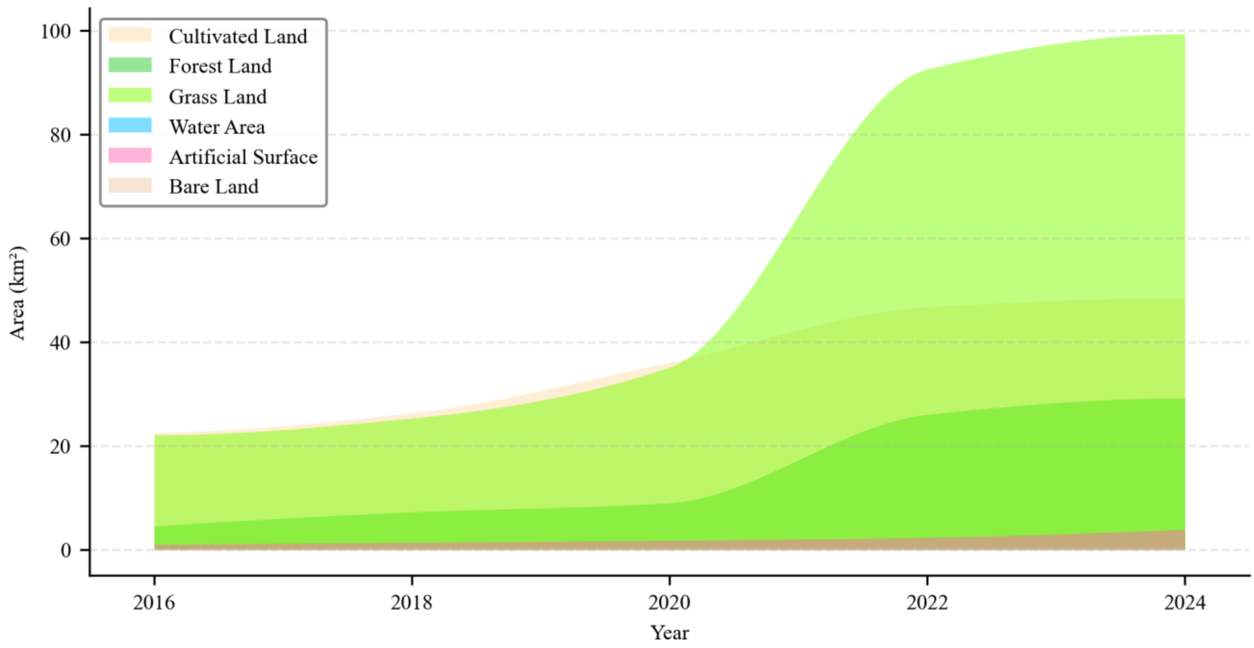

Figure 5. Area of land cover types occupied by wind farms in the study area

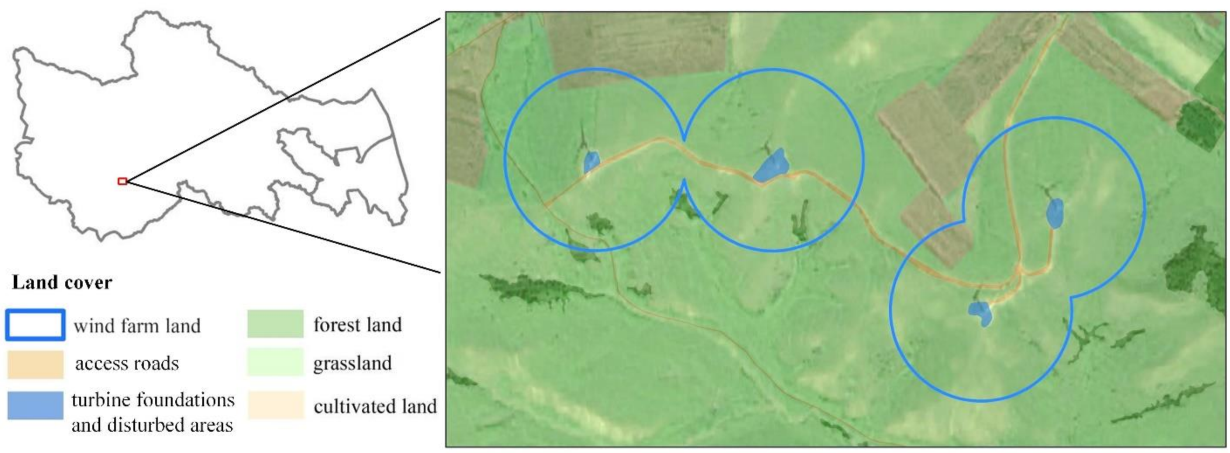

Figure 6. Spatial schematic of land cover types in a localized wind farm area.

Artificial surface expanded steadily by +21.03 km² (+4.73%, LK= +0.59%/yr). Minor increases were also observed in bare land (+8.93 km², LK = +2.02%/yr) and water areas (+7.08 km², LK = +0.16%/yr). Among the declining categories, grassland experienced the greatest absolute reduction of −101.29 km² (−1.21%), with an annual dynamic degree (LK) of −0.15%/yr. Despite its large spatial extent (8,348.7 km² in 2016), grassland exhibited a sustained and progressive decline across all monitoring intervals. Forest land decreased by −49.18 km² (−1.06%, LK = −0.13%/yr). Cultivated land showed the smallest net decline among the reduced categories (−17.44 km², −0.35%, LK = −0.04%/yr).

4.1.2 Period-wise Changes: As illustrated in Figure 3, the land cover changes in the study area across four two-year intervals from 2016 to 2024 exhibit distinct spatiotemporal characteristics. Grassland, forest land, and cultivated land show continuous decreasing trends throughout the study period. Grassland experienced substantial reductions in all intervals, declining by 30.1 km², 25.3 km², 23.4 km², and 22.5 km² during 2016–2018, 2018–2020, 2020–2022, and 2022–2024, respectively, with a pattern of decreasing magnitude but consistently negative values. Forest land losses were concentrated in the first two intervals (2016–2020), with declines moderating thereafter. Cultivated land showed relatively smaller reductions, averaging approximately −4.3 km² per interval. Wind farm land represents the most dramatic change. The interval 2020–2022 witnessed the most intense expansion, with an increase of 85.83 km²—the peak value over the study period. Growth during 2016–2018, 2018–2020, and 2022–2024 amounted to 10.16 km², 21.66 km², and 13.22 km², respectively.

4.1.3 Land Cover Transitions: In terms of major transition pathways (Figure 4), the conversion from grassland to wind farm land represents the most prominent change process, with a transition area of 78.74 km²—the largest among all off-diagonal transitions—indicating that grassland served as the primary spatial source for wind farm expansion. This was followed by forest land to cultivated land (34.27 km²), grassland to cultivated land (26.49 km²), and cultivated land to wind farm land (26.48 k-

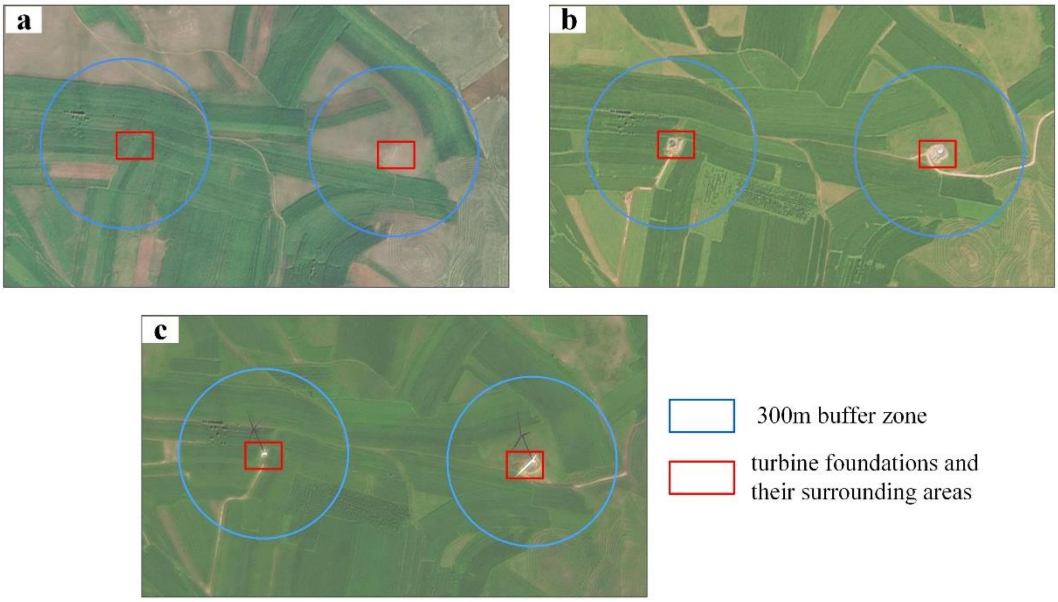

Figure 7. Temporal dynamics of land cover composition within wind farm areas. (a) pre-construction (2016); (b) mid-construction (2020); (c) post-construction (2024).

m²). Additionally, the transition from forest land to wind farm land reached 24.19 km², further illustrating that wind farm development has resulted in notable occupation of both natural ecological land and certain productive land. Regarding the source composition of wind farm land in 2024, apart from the persistence of existing wind farm land, the newly added area originated mainly from grassland, cultivated land, and forest land. Among these, grassland contributed 59.66% of the newly added wind farm land, while cultivated land and forest land accounted for 20.06% and 18.33%, respectively. These findings show that wind farm expansion first occurred in grassland landscapes, accompanied by the conversion of certain cultivated and forest lands into energy infrastructure land.

4.2 Analysis of Land Occupancy Types for Wind Farms

4.2.1 . Land Cover Areas Occupied by Wind Farms: Grassland was the dominant land cover type within wind farm buffer zones throughout the study period (Figure 5). Its area increased from 22.08 km² in 2016 to 99.30 km² in 2024, representing a net gain of 77.22 km² (+349.8%). Notably, grassland accounted for 54.8% of total wind farm land by 2024, up from 43.9% in 2016. Cultivated land was the second largest contributor to wind farm land, expanding from 22.49 km² (44.7% of total in 2016) to 48.42 km² (26.7% in 2024). Forest land showed the highest relative growth rate among the major land cover types, increasing from 4.53 km² to 29.16 km² (+543.9%). Within the areas designated for wind farm development, the composition of land surface cover transitioned from a balanced state of cultivated land and grassland to a grassland-dominated configuration.

4.2.2 Impacts of Wind Farm Development on Land Cover: Figure 6 intuitively illustrates the alterations in land surface cover induced by wind farm construction, which are primarily manifested in the turbine foundations and their surrounding areas, the access roads between turbines, and other associated infrastructure. Specifically, turbine foundations are directly converted from cultivated land, grassland, or forest land to artificial surface. Meanwhile, the land surface within approximately 30 m of the turbine foundations is disturbed by construction activities, resulting in temporary landcover changes. Figure 7 presents the land cover changes before and after the construction period, showing that the disturbed surfaces gradually recover: cultivated land recovers relatively quickly, whereas grassland recovers more slowly. Furthermore, due to the ongoing need for operation and maintenance access, the land cover types of the internal roads within the wind farm generally do not undergo further change.

5. Conclusion

The aim of the study has been to analyse the spatio-temporal changes in land cover of wind farms within county areas. The obtained results are listed as follows.

(1) From 2016 to 2024, the composition of land cover classes underwent notable changes driven primarily by wind farm expansion, representing a cumulative increase of 130.87 km² (+260.35%) and the highest dynamic degree among all categories (LK = +32.54%/yr). Outside the wind farm land, artificial surfaces and water bodies exhibited an increase, whereas ecological and agricultural land cover types, specifically cultivated land, forest land, and grassland, displayed a decreasing trend.

(2) Grassland was the most impacted land cover type, exhibiting the most pronounced transition to wind farm land. This conversion amounted to 78.74 km², representing 59.66% of the newly established wind farm land, whereas cultivated land and forest land accounted for 20.06% and 18.33%, respectively.

(3) In 2016, wind farm land was composed mainly of cultivated land (44.75%) and grassland (43.92%). By 2024, the cultivated land share had dropped to 26.73%, whereas grassland increased to 54.82%. As wind power expanded, the composition of wind farm land shifted from a cultivated land–grassland balance toward grassland dominance.

(4) The construction of wind farms, including turbine foundations, access roads, and associated infrastructure, directly modifies land surface cover types. Areas subject to temporary disturbance from construction activities tend to recover progressively, with cultivated land exhibiting a faster recovery rate than grassland.

This study provides only a preliminary statistical analysis of the status of wind energy construction land and regional land cover changes. Several limitations remain to be addressed in future research. First, the delineation of wind farm boundaries in this study was based solely on a 300 m buffer zone around individual wind turbines, which is a simplification that does not account for numerous other relevant factors. Second, the analysis lacks an assessment of the ecological and environmental impacts associated with wind farm development. These issues warrant further investigation in subsequent studies.

Acknowledgements

This work was financially supported by the National Key Research and Development Program of China: Intelligent extraction and development potential assessment technology of wind power and photovoltaic power station target information (No.2022YFF1303401).

References

Aristides, M., Panagiotis, G., Elzbieta, K., Eleftherios, K., 2023. Wind turbine power and land cover effects on cumulative bat de aths. The Science of the total environment,892,164536-164536.

Aydin, N.Y., Kentel, E., & Duzgun, S. (2010). GIS-based enviro nmental assessment of wind energy systems for spatial planning : A case study from Western Turkey. Renewable & Sustainable Energy Reviews, 14, 364-373.

Chen, X., Xie, L., Zhang, X., Li, Y., 2025. Land use impacts the environmental benefits of wind energy farms in China. Commu nications Earth & Environment. https://doi.org/10.1038/s43247-025-02833-w.

Denholm, P.L., Hand, M., Jackson, M.E., & Ong, S. (2009). Lan d Use Requirements of Modern Wind Power Plants in the Unite d States. A national laboratory of the U.S. Department of Energ yOffice of Energy Efficiency & Renewable Energy.

Deng, Y., Zhang, H., Wang, J., Liu, Q., 2025. Land-use require ments and occupancy patterns of rapidly expanding wind farms in China. Environmental Research Letters. https://doi.org/10.10 88/1748-9326/add7ee.

Fei, T., Lu, D., Li, Y., Li, D., Tian, S., Amar, A., Yang, X., Li, Z ., 2025. The impact of the wind farm on the vegetation and the microclimate via remote sensing: a case study in Hebei Province , China. Energy, Ecology and Environment. https://doi.org/10.1 007/s40974-025-00386-4.

Han, X., Lu, C., Wang, J., 2025. Long-term impacts of 250 wind farms on surface temperature and vegetation in China: a remote sensing analysis. Remote Sensing, 17(1): 10. https://doi.org/10. 3390/rs17010010.

IEA (International Energy Agency), 2024. Renewables 2023. htt ps://www.iea.org/reports/renewables-2023.

Jia, Z., Yang, X., Chen, A., Yang, D., Zhang, M., Wei, L., 2024. Localized eco-climatic impacts of onshore wind farms: a review Journal of Resources and Ecology, 15(1): 151–160. https://doi.o rg/10.5814/j.issn.1674-764x.2024.01.013.

Korozi, O., Vagiona, D., 2024. Environmental Impact Assessme nt of Onshore Wind Farms in the Region of Central Greece Usin g a Modified RIAM Method. Journal of Environmental & Earth Sciences,6(1), 6173.

Kumar, A., HE, X., Deng, Y., Sah, B., Singh, A., Kumar, P., Kir tley, J., 2025. Earth Grid: Toward a low-carbon energy infrastru cture. iScience, 28(11):113681-113681.

Li, D., Ma, C., Yue, C., Lin, N., Zhu, Y., Wu, J., 2024.Windfar m construction alters soil multinutrient cycling by destabilizing microfauna community in a mountain ecosystem. Journal of env ironmental management, 373, 123758.

Liu, J., Lin, Y., Jiang, M., Guo, X., 2024. Exploring policy supp ort for wind power development from a balancing perspective - A study of dynamic strategies based on evolutionary game. Ener gy Policy, 188114061.

Liu, L., Wang, Y., Wang, Z., Li, S., Li, J., He, G., Li, Y., Liu, Y., Piao, S., Gao, Z., Chang, R., Tang, W., Jiang, K., Wang, S., Wa ng, J., Zhao, L. and Chao, Q., 2022. Potential contributions of w ind and solar power to China's carbon neutrality. Resources, Co nservation and Recycling, 180: 106155.

Sun, Y., Li, Y., Wang, R., Ma, R., 2024. Modelling potential lan d suitability of large-scale wind energy development using expla inable machine learning techniques: applications for China, US A and EU. Energy Conversion and Management, 302: 118131. h ttps://doi.org/10.1016/j.enconman.2024.118131.

Yang, X., Liu, H., Qin, Z., Li, A., 2016. Monitoring wind farms occupying grasslands based on remote-sensing data from China' s GF-2 HD satellite: a case study of Jiuquan City, Gansu Provin ce, China. Ecological Engineering, 91: 220–229. https://doi.org/ 10.1016/j.ecoleng.2016.03.015.

Zhang, L., Fan, L., Ma, C., Liu, J., Zhu, Y., Chen, Z., Wu, J., 20 22. Influence of mountain wind farm construction on soil proper ties and vegetation cover: a case study of Jiangjunshan wind far m in Yunnan Province. Chinese Journal of Ecology, 41(12): 239 7–2405. https://doi.org/10.13292/j.1000-4890.202212.010.

Zhao, X., Li, F., Yuan, Y., Ari, G., Yan, Y., Zhang, Q., Olhnuud , A., Liu, P., 2025. Wind farms reduce grassland plant communi ty diversity and lead to plant community convergence. BMC Ec ology and Evolution, 25(1): 10. https://doi.org/10.1186/s12862-025-02350-6.

Zhu, R., Li, X., Zhang, W., Wang, Y., 2023. The impact of onsh ore wind farms on ecological connectivity: a landscape-scale an alysis using least-cost path modeling. Environmental Research Communications, 5(1).